

Spontaneous Symmetry Breaking Facilitates Metal-to-Ligand Charge Transfer: A Quantitative Two-Photon Absorption Study of Ferrocene-phenyleneethynylene Oligomers

Alexander Mikhaylov,[†] Merle Uudsemaa,[‡] Aleksander Trummal,[‡] Eduardo Arias,[§] Ivana Moggio,[§] Ronald Ziolo,[§] Thomas M. Cooper,^{||} and Aleksander Rebane^{*,†,‡,§,||}

[†]Department of Physics, Montana State University, Bozeman, Montana 59717, United States

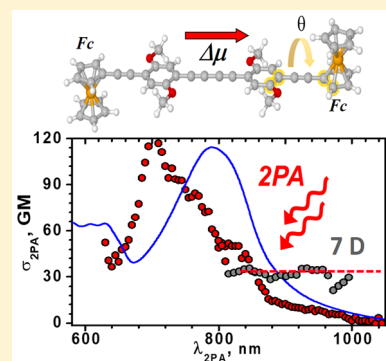
[‡]National Institute of Chemical Physics and Biophysics, 12618 Tallinn, Estonia

[§]Centro de Investigación en Química Aplicada (CIQA), 25294 Saltillo, Coahuila, Mexico

^{||}Materials and Manufacturing Directorate, Air Force Research Laboratory, Wright-Patterson Air Force Base, Ohio 45433, United States

Supporting Information

ABSTRACT: Change of the permanent molecular electric dipole moment, $\Delta\mu$, in a series of nominally centrosymmetric and noncentrosymmetric ferrocene-phenyleneethynylene oligomers was estimated by measuring the two-photon absorption cross-section spectra of the lower energy metal-to-ligand charge-transfer transitions using femtosecond nonlinear transmission method and was found to vary in the range up to 12 D, with the highest value corresponding to the most nonsymmetric system. Calculations of the $\Delta\mu$ performed by the TD-DFT method show quantitative agreement with the experimental values and reveal that facile rotation of the ferrocene moieties relative to the organic ligand breaks the ground-state inversion symmetry in the nominally symmetric structures.



Ferrocene-based complexes possess intriguing nonlinear optical and charge-transport properties, which make them subject to continuing research.^{1–4} A prominent feature of the UV–vis absorption spectrum of the numerous organometallic complexes of ferrocene (Fc) consists of a broad red-shifted band (or bands) associated with metal-to-ligand charge-transfer (MLCT) transitions,^{5–18} where a notable fraction of the electron density shifts from the Fe atom(s) in the ground electronic state toward the organic group(s) in an excited state. MLCT transitions are associated with a large change of the molecular permanent electric dipole moment, $\Delta\mu$ (up to 30 debye, D⁷), that, in turn, is instrumental for achieving high second-order nonlinear susceptibility^{1,6,13,17} and also contributes to charge separation and charge-transport properties.^{19–23} Interestingly, prominent first hyperpolarizability is routinely observed not only in noncentrosymmetric organometallic structures but also in nominally centrosymmetric structures.^{12,17,24,25} Such obvious spontaneous symmetry breaking was tentatively associated with steric distortions of the ground-state molecular structure,^{24,26} even though quantitative explanation has so far been lacking.

In this Letter, we shed light on the origin of the symmetry breaking effect by experimentally evaluating the $\Delta\mu$ value in a series of ferrocene-phenyleneethynylene oligomers in THF solution comprising both nominally centrosymmetric as well as noncentrosymmetric structures and by comparing the exper-

imental results with TD-DFT calculations that account for possible facile rotations within the complex. Figure 1 shows the chemical structures of 10 systems studied in this work including the unmodified ferrocene 1, six noncentrosymmetric compounds 2–7 carrying one ferrocene unit, and three nominally centrosymmetric structures 8–10, where the two peripheral ferrocene moieties are linked by a conjugated chain of a varying length. The ferrocene moieties are acting as electron donors (D), whereas 2,5-di(alkoxy)-benzeneethynylene(s) is used as a π -conjugated linker (π) and benzyl benzoate or benzoic acid acting as termini and electron attractor groups (A), thus creating an intramolecular charge transfer (ICT) system (D– π –A). Details of the oligomer 2–10 synthesis along with a comprehensive chemical characterization of the compounds are presented in the Supporting Information.

Because solvatochromic techniques²⁷ commonly used for the determination of $\Delta\mu$ rely on measuring the fluorescence spectrum, and in view of the fact that the MLCT chromophores lack appreciable fluorescence emission, accurate experimental evaluation of the $\Delta\mu$ posed certain challenges. Probing the solvent polarity dependence of the linear absorption spectra

Received: February 16, 2018

Accepted: March 27, 2018

Published: March 27, 2018

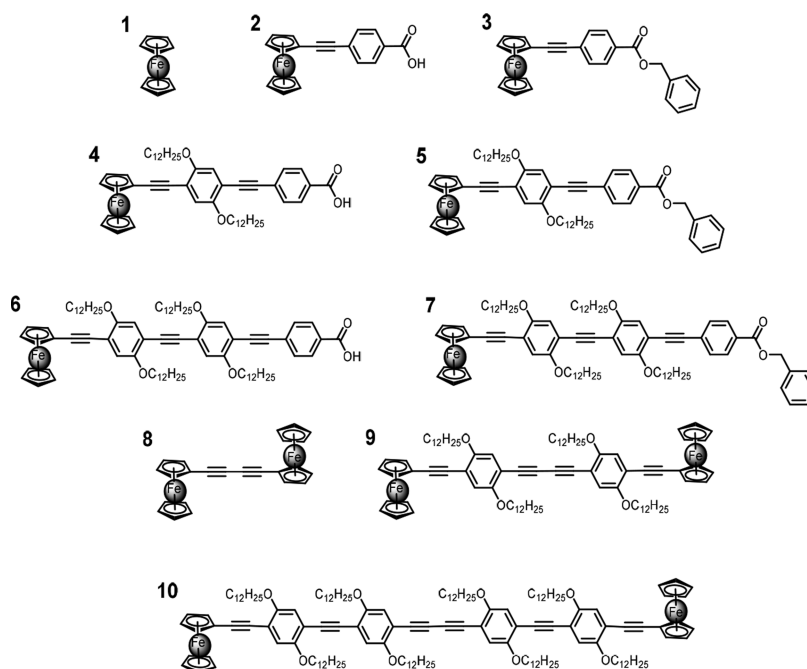


Figure 1. Chemical structures of the studied ferrocene-phenyleneethynylene oligomers.

may give an estimate of the ground-state dipole moment but does not reveal the amount of charge transferred in the vertical transition. Electroabsorption spectroscopy (EAS), also called Stark spectroscopy, allows the estimation of $\Delta\mu$ based on how the linear absorption spectrum changes upon application of external electric field (see, e.g., ref 28). However, if the MLCT band contains multiple overlapping transitions,^{6–17,29} then quantitative interpretations of such measurements may be less than straightforward.³⁰ Furthermore, EAS experiments are typically carried out in a dielectric medium such as polymers and glasses, where the actual (local) static electric field strength acting on the chromophore differs from the externally applied voltage by an inadequately specified correction factor,³¹ thus increasing the uncertainty of the $\Delta\mu$ value.²⁸

To alleviate the above listed complications, we use an alternative experimental approach based on quantitative measurement of the instantaneous two-photon absorption (2PA) cross section, σ_{2PA} . According to well-known two essential states (2ES) approximation (also called two-level model) of 2PA, the $\Delta\mu$ (in statcoulomb-cm) may be related to the 2PA cross section of the same transition as follows (see the Supporting Information)

$$|\Delta\mu| = \left(\frac{5}{12 \times 10^3 \pi \ln 10} \frac{nc^2 h N_A \sigma_{2PA}}{f^2 \epsilon \lambda_{1PA}} \right)^{1/2} \quad (1)$$

where σ_{2PA} is the 2PA cross section (in $\text{cm}^4 \cdot \text{s}$), c is the speed of light (in $\text{cm} \cdot \text{s}^{-1}$), h is the Planck constant (in $\text{erg} \cdot \text{s}$), $f = (n^2 + 2)/3$ is the optical local field correction factor, ϵ is the molar extinction coefficient (in $\text{M}^{-1} \text{cm}^{-1}$), λ_{1PA} is the 1PA transition wavelength (in cm), and N_A is the Avogadro constant. This relation, if applied to the lowest energy transition in the case where 1PA and 2PA profiles coincide, offers an estimate of $\Delta\mu$ without the application of external electric field and was recently implemented for the study of organic ICT chromophores³² as well as some Pt–organic complexes.^{33,34} Here we use nonlinear transmission (NLT) method to experimentally determine the σ_{2PA} in the excitation wavelength

range $\lambda_{2PA} = 620\text{--}1050$ nm (for details, see the Supporting Information). By combining the 2PA data with the corresponding one-photon absorption (1PA, or molar extinction) spectrum in the range 310–525 nm, we determine $\Delta\mu$ by applying the eq 1. Figure 2 shows the measured 2PA spectra (black empty symbols, lower wavelength scale) in $\lambda_{2PA} = 620\text{--}1050$ nm range, along with the corresponding linear molar extinction spectra (blue solid line, upper wavelength scale) for compounds 1–10. Estimated experimental error of the 2PA data is $\sim 30\%$.

The 1PA spectrum of unsubstituted ferrocene 1 displays two lower energy bands spanning the $\lambda_{1PA} = 300\text{--}550$ nm range (Figure 2 a) with low peak values, $\epsilon_{\text{max}} < 10^2 \text{ M}^{-1} \text{cm}^{-1}$. Previous studies assign the lowest energy band at 440 nm to a $d\text{--}d^*$ transition, while MLCT is located at 325 nm.^{17,18} The estimated σ_{2PA} value was on the level of or below our detection sensitivity, $\sigma_{2PA} < 0.1 \text{ GM}$, thus offering only an upper limit estimate, $\Delta\mu < 10 \text{ D}$. Equation 1 provides us with an upper limit estimate for the dipole moment change, $\Delta\mu < 10 \text{ D}$. To our best knowledge, there are no previous reports on σ_{2PA} or $\Delta\mu$ values of the unsubstituted ferrocene. Linking ferrocene with phenyl carboxylic acid (2) or benzyl benzoate (3) groups significantly intensifies the low-energy part of the 1PA spectrum ($\epsilon_{\text{max}} \approx (1 \text{ to } 4) \times 10^3 \text{ M}^{-1} \text{cm}^{-1}$) while shifting the corresponding absorption peaks slightly to the red (Figure 2b,c). Following Barlow et al.⁵ we call the two longest wavelength bands LE1 and LE2 and the stronger ($\epsilon_{\text{max}} \approx (1.5 \text{ to } 2) \times 10^3 \text{ M}^{-1} \text{cm}^{-1}$) band at higher energy ($\lambda_{1PA} = 270\text{--}320$ nm) the HE band. The 2PA spectra of 2 and 3 both show two distinct features, centered at 900–960 and 680–720 nm, with the corresponding peak values, $\sigma_{2PA} \approx 1$ to 2 GM and 10–13 GM (LE1 and LE2, respectively). According to the 2ES model, the shape of the 2PA spectrum should match that of the corresponding 1PA transition spectrum.³²

To confirm which part of the measured 2PA spectra corresponds to particular MLCT transition in the 1PA spectra, we evaluate eq 1 for the whole wavelength range. The results

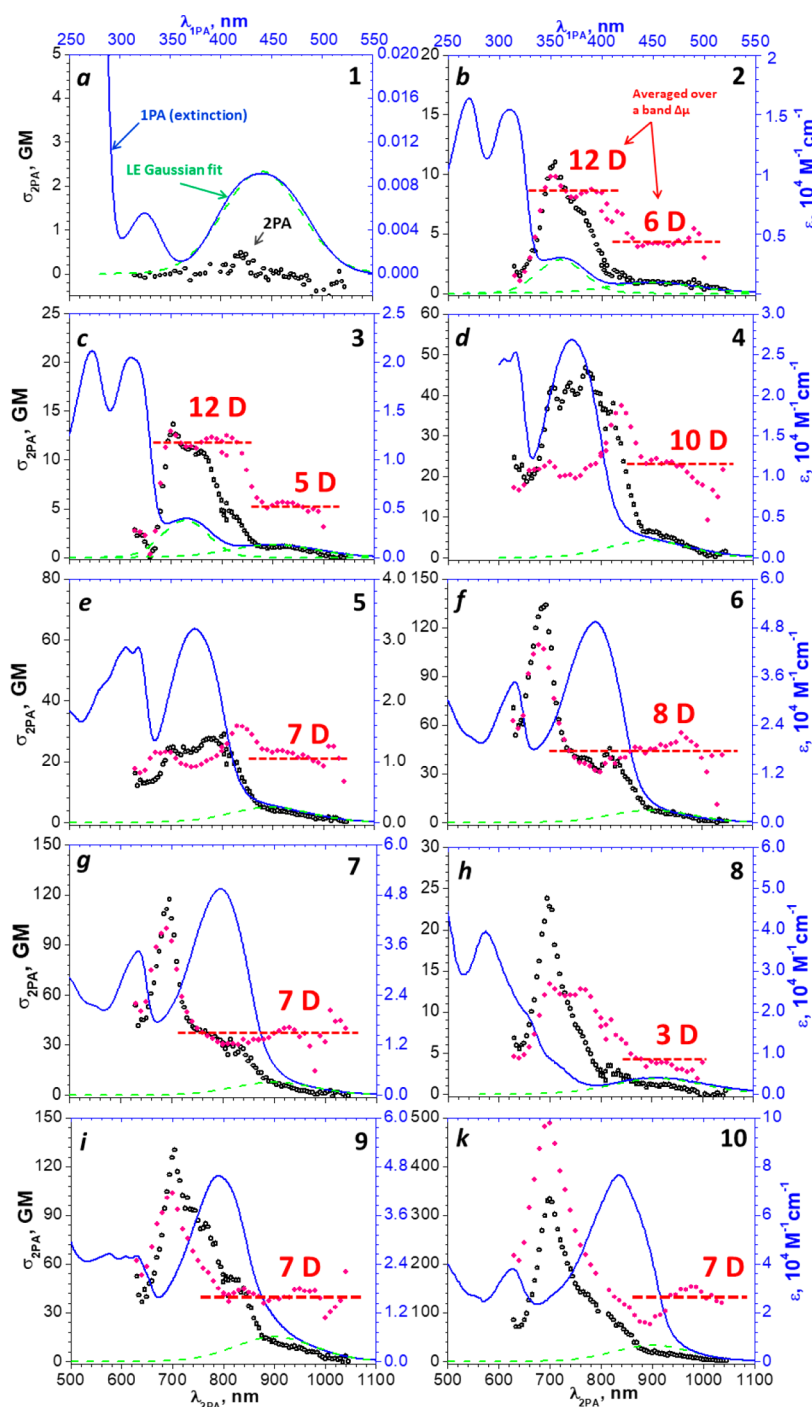


Figure 2. Two-photon absorption (2PA) and one-photon absorption (IPA) spectra of compounds **1–10** (a–k). Left vertical axes (scaled in Goeppert Mayer, GM) represent 2PA cross sections, σ_{2PA} (black empty symbols), and right vertical axes (scaled in $M^{-1} \text{ cm}^{-1}$ units) show the corresponding extinction coefficients, ϵ (blue solid line). Lower (upper) horizontal scales correspond to the two-photon, λ_{2PA} (one-photon, λ_{1PA}), excitation wavelengths. The horizontal axes are scaled identically on all graphs. Gaussian fits for the lower energy (LE1 and where it is possible LE2) 1PA bands are shown by dashed green lines. Change of permanent dipole moments between the ground and first excited states, $\Delta\mu$, evaluated from eq 1 for each wavelength (a profile) is shown by red dots (not to scale); averaged over LE band wavelength ranges (the regions showed by red dashed lines) $\Delta\mu$ values are indicated in debye, D, units (red numbers).

are presented in Figure 2 as red dot symbols. The fact that the $\Delta\mu$ profile is nearly constant for both LE1 and LE2 bands (dashed horizontal lines) indicates that the 2ES model may be applicable to both of these bands. Quantitatively, eq 1 yields for the LE1 band of **2** and **3**, respectively, $\Delta\mu \approx 6$ and 5 D, whereas the LE2 band values are about twice as large, $\Delta\mu \approx 11$ and 12 D. In the case of the remaining four nonsymmetric compounds

4–7, the HE transitions in 1PA spectrum continue to gain slightly in intensity and experience a further bathochromic shift (Figure 2d–g), which is in accord with the previously noted behavior of interligand charge transfer (ILCT) excitations upon extension of π -conjugation.^{5,10,17} At the same time, the relatively weak LE1 band shows no noticeable shift. This leads to a substantial overlap between different spectral

components, rendering the LE1 transition to appear merely as a broad shoulder on the red side of a much stronger band, while HE and LE2 bands practically overlap. In an effort to retrieve the shape of the LE1 components, we fitted the long-wavelength shoulder of the 1PA spectrum with a Gaussian (green dashed lines on Figure 2) and used these fits to determine the corresponding peak wavelengths and the ϵ_{\max} value for the LE1 transitions. The corresponding $\Delta\mu$ values vary in the range 7–10 D (Table 1). Among the three

Table 1. Summary of Two-Photon Absorption (2PA) and One-Photon Absorption (1PA) Properties of the Studied Compounds: Measured σ_{2PA} and $\Delta\mu$ Values Obtained from Equation 1, $\Delta\mu^{\text{exp}}$, and Derived from the TD-DFT Calculations, $\Delta\mu^{\text{calc}}$, Corresponding to the MLCT Transitions in LE Bands (LE1 and LE2) at λ_{1PA} Wavelengths

compound	band	λ_{1PA} (nm)	σ_{2PA} (GM)	$\Delta\mu^{\text{exp}}$ (D)	$\Delta\mu^{\text{calc}}$ (D)
1	LE1	441	<0.1	<10	
Nonsymmetric					
2	LE1	450	2	6	6.2 ^a
	LE2	360	10	12	12.8 ^a
3	LE1	450	1	5	5.7 ^a
	LE2	360	13	12	13.0 ^a
4	LE1	450	6	10	9.0 ^a
5	LE1	450	4	7	8.1 ^a
6	LE1	450	9	8	9.5 ^a
7	LE1	450	7	7	8.7 ^a
Centrosymmetric					
8	LE1	450	1	3	0.3 ^b
9	LE1	450	13	7	7.4 ^b
10	LE1	450	17	7	2.7 ^b

^aCalculated for the global minima energy configuration. ^bCalculated for rotamers representing local minimum within 0.4 kT above the global energy minima ($\theta = 16, 95,$ and 89° rotations from the centrosymmetric positions for compounds 8, 9, and 10, respectively).

nominally centrosymmetric compounds, 9 and 10 show linear absorption spectra in the long wavelength range (Figure 2i,k) that closely resemble the nonsymmetric chromophores 6 and 7. Using eq 1, we arrive at a quantitatively similar large $\Delta\mu \approx 7$ D for the LE1 band. The ligand of compound 8 has the shortest conjugation pattern among the nominally symmetric structures. Accordingly, here the LE1 band is still well separated from the rest of the spectrum (Figure 2 h), yielding $\Delta\mu \approx 3$ D. All values are summarized in Table 1.

At this point one might question the applicability of eq 1 to nominally symmetric systems. To clarify this issue, let us consider 1D particle-in-a-box model with infinite walls. If the bottom of the potential is flat, then all even-numbered energy eigenstates, starting with the ground state, are gerade, while all odd-numbered states starting with the first excited state are ungerade. One-photon electric dipole transitions between any pair of opposite parity levels is allowed, while corresponding two-photon transition is strictly forbidden. Note that this exclusion applies equally to all terms in the sum-over-states (SOS) expression of the 2PA cross section. Indeed, the two-level term vanishes because permanent dipoles are zero, and all three-level terms vanish because one of the transitions connected to the intermediate level is zero. If we would slightly disturb the inversion symmetry, for example, by tilting the bottom potential, then the formally forbidden two-photon transition between opposite parity states becomes partially

allowed, while, at same time, the corresponding one-photon transition undergoes no significant change. To the best of our knowledge, there is currently no mathematical formalism that would predict which of the two alternative two-photon paths makes the largest contribution. Our above use of eq 1 in 8–10 relates to the previous studies showing that two-level system (2LS) contribution prevails for the 0–0 transition in nominally symmetric Pt-acetylides.^{33,34}

Our TD-DFT calculations performed on the ferrocene-phenyleneethynylene oligomers (see Supporting Information for details) reproduced well the main feature of the 1PA spectra and confirmed the MLCT origin of the LE1 bands being affiliated with S_0-S_2 and S_0-S_1 transitions in the case of compounds 2, 3, and 8, and 4–7, 9, and 10, respectively, and the ILCT type transitions associated with the HE bands. At the same time, intermediate bands LE2 are formed as either MLCT (compounds 2 and 3) or some combination of both MLCT and ILCT transitions (compounds 4–10). The simulations also revealed an excellent correlation with the experimental $\Delta\mu$ values in the case of noncentrosymmetric compounds 2–7 (Table 1). For oligomers 2 and 3, the calculated $\Delta\mu$ values for both LE1 and LE2 bands are in quantitative agreement with the experiment. We can say the same about the LE1 transitions in the case of compounds 4–7. A similar comparison for the higher energy transitions indicates that $\Delta\mu$ may reach even higher values up to 19 D (see Supporting Information). It is reasonable to assume that the nonvanishing $\Delta\mu$ in 8–10 is most likely due to spontaneous lowering of the symmetry.³⁵ Because both 1PA and 2PA are instantaneous vertical excitation processes, any possible lowering of symmetry associated with excited-state relaxation may be excluded.³⁶ Thus we conclude that the symmetry must be broken in the equilibrium ground state.

Recently, Cooper et al. showed that some nominally nearly symmetric linear Pt-acetylides possess large $\Delta\mu$ up to 25 D due to twisting of the ligands.³³ Kaur et al. developed a similar model to explain origin of nonzero $\Delta\mu$ in symmetric ferrocene-diketopyrrolopyrrole triads due to distortions of the ferrocene units, but no quantitative match with the experiment was found.²⁴ To elucidate the origin of the symmetry breaking, we calculated the dependence of ground state energy and $\Delta\mu$ on some asymmetric conformation changes most likely to occur in THF. Figure 3 presents the calculated ground state energy of 9 for different rotation angles of one of the two ferrocene moieties relative to the rest of the structure ($\theta = 0^\circ$ corresponds

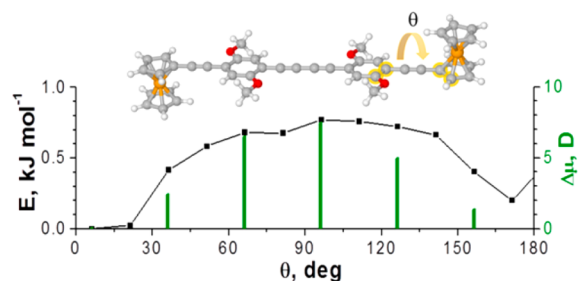


Figure 3. Rotational distortions in compound 9 that result in the appearance of $\Delta\mu$ in the ground state. Upper panel defines the rotational angle θ . Lower panel shows the angular dependence of the $\Delta\mu$ (right vertical axis scaled in D) and energy barriers E for the conformers relative to the global minimum (left vertical axis scaled in kJ mol^{-1}).

to the centrosymmetric conformation shown in Figure 1). The different ground-state rotational conformations occur with a low energetic cost less than ~ 0.4 kT (1 kJ mol^{-1}), giving rise to surprising large $\Delta\mu$ values. The maximum $\Delta\mu = 7.4$ D is achieved at $\theta = 95^\circ$, which is in excellent agreement with the experiment (Table 1). A comparable behavior was observed for the compounds **8** and **10**, comprising, respectively, a reduced and extended conjugated chain length: Appreciable $\Delta\mu$ is induced by the rotation of the ferrocene units with low energetic cost (Table 1 and the Supporting Information).

Tables S19 and S20 in the Supporting Information summarize the 2PA strengths calculated using the DALTON program package. Comparing these values to our experimental findings in Table 1 reveals that in **9** the 2PA in the MLCT transition of a distorted conformation with 90° rotated ferrocene unit is close to 100%, determined by the $\Delta\mu$ parameter. The low-energy region comprises at least four transitions about 20 nm apart, with the lowest energy one contributing the most both to 1-photon oscillator strength and 2PA probability. In the conformer of **10** with the rotated Fc group, there are five transitions within the 50 nm range, with the lowest energy component containing $\sim 32\%$ of the 2PA transition probability, whereas the nearby 1-photon-prohibited but 2-photon-allowed transition carries twice as much of 2PA strength (64%). The calculation places this transition at about 40 nm shorter wavelength, which is comparable to or even less than average observed bandwidth. On the contrary, the experimentally determined ratio between 2PA and 1PA spectra (Figure 2) stays more or less constant in the 850–1050 nm range, which could indicate that the SOS-allowed band in question may, in fact, be located at even shorter wavelengths. Because of these two potential contributions, the actual $\Delta\mu$ may be smaller than the value estimated from eq 1, 7 D. In case of **8** the calculation showed four transitions in narrow 8 nm range, none of which possess appreciable 1-photon oscillator strength, independent of the conformation. Here the 2-photon transition probability is almost entirely due to SOS-type contributions, none of the excited states showing appreciable $\Delta\mu$ value. This could represent a situation where eq 1 is not applicable. However, it remains puzzling why the 2-photon spectrum still follows closely the linear absorption profile. It is possible that due to close proximity on the energy scale, the excited states are actually acting as a superposition state, thus further complicating theoretical analysis. To account for this newly revealed uncertainty, we call the experimental $\Delta\mu$ the maximum estimated value. The fact that in **10** the calculated $\Delta\mu$ is a factor of ~ 2 lower than the observed experimental value could be also related to additional degrees of flexibility associated with benzeneethynylene ring rotations^{37–42} (see the Supporting Information). It is worth noting that a recent computational study of nominally symmetric polymethine dyes revealed the dependence of ground-state symmetry breaking on bond-length alternation and conjugated chain length.⁴³ Even though lowering of symmetry in ferrocene oligomers also correlates with the conjugation length, our systems carry no ground-state charge and exhibit no resonating structures.

Still another way to verify our finding is to note that experimental literature already offers a trove of second- and third-order nonlinear optical (NLO) properties of a variety of organometallic systems measured by z-scan^{12,25,43} and hyper-Rayleigh scattering (HRS)^{7,11,15,16} methods. It presents interest to recast the previous experimental results to reveal the underlying $\Delta\mu$ values in a similar manner as was presented

above regarding our NLT measurements. Table S22 in the Supporting Information summarizes the $\Delta\mu$ that we derived using the previously published NLO data. In a good agreement with our current findings, the values reach 20 D for nominally centrosymmetric systems and 30 D for nonsymmetric systems (see the Supporting Information for details). For example, in ferrocene- α -cyanostilbene that is structurally related to our compound **9**, we estimate based on the second-order nonlinear polarizability value determined by Dhoun et al.,⁴⁴ $\Delta\mu = 4.5$ D. Our calculations give $\Delta\mu = 7.5$ to 9.2 D depending on the rotation angle, thus lending support to the notion of rotationally deformed ground state (see Table S21 in the Supporting Information for details). In the case of nominally symmetric ferrocene-diketopyrrolopyrrole dyads studied by Kaur et al.,²⁴ our calculations also lead to remarkable increase in $\Delta\mu$ with increasing rotational distortions; however, more accurate quantitative comparison was hindered due to a substantial overlap between the MLCT bands and the red-shifted ILCT transitions.

In summary, we measured experimentally and calculated theoretically the change of electric dipole moment in low-energy transitions of a series of new symmetric and nonsymmetric ferrocene-phenyleneethynylene oligomers. On the basis of good agreement between the calculated and experimental values, we conclude that rotational distortions can break the ground-state symmetry in the formally symmetric compounds, thus leading to large $\Delta\mu$ values. To our best knowledge, this is the first time that the physical origin of nonvanishing dipole moment in MLCT transitions of symmetric organometallic complexes has been quantitatively characterized. Our results improve basic understanding of the MLCT process and can facilitate the development of new organometallic systems with augmented NLO and charge-transport properties. Our results also validate using 2PA as an alternative to the traditional methods of measuring molecular dipole moments in condensed environments.

■ ASSOCIATED CONTENT

Supporting Information

The Supporting Information is available free of charge on the ACS Publications website at DOI: 10.1021/acs.jpcllett.8b00525.

Information about the chemical compounds synthesis and characterizations along with details of used calculations and experimental method (PDF)

■ AUTHOR INFORMATION

Corresponding Author

*E-mail: arebane@montana.edu.

ORCID

Aleksander Trummal: 0000-0002-2943-6129

Thomas M. Cooper: 0000-0002-4635-8281

Aleksander Rebane: 0000-0003-4330-5544

Notes

The authors declare no competing financial interest.

■ ACKNOWLEDGMENTS

This work was supported by Ministry of Education and Research, Republic of Estonia (grants IUT23-9 and IUT23-7), European Regional Development Fund (project TK134), and AFOSR (grant FA9550-16-1-0189). T.M.C. is thankful to D. Stewart for extinction coefficients determination.

REFERENCES

- (1) Ghosal, S.; Samoc, M.; Prasad, P. N.; Tufariello, J. J. Optical Nonlinearities of Organometallic Structures: Aryl and Vinyl Derivatives of Ferrocene. *J. Phys. Chem.* **1990**, *94*, 2847–2851.
- (2) Togni, A.; Hayashi, T. *Ferrocenes: Homogeneous Catalysis, Organic Synthesis, Material Science*; VCH Verlagsgesellschaft, Weinheim (FRG) and VCH Publisher: New York, 1995.
- (3) Debroy, P.; Roy, S. Recent Advances in the Synthesis and Properties of Ferrocenes Having an Unsaturated Backbone. *Coord. Chem. Rev.* **2007**, *251* (1–2), 203–221.
- (4) Stepnicka, P. *Ferrocenes: Ligands, Materials and Biomolecules*; John Wiley and Sons, Ltd.: Chichester, England, 2008.
- (5) Barlow, S.; Bunting, H. E.; Ringham, C.; Green, J. C.; Bublitz, G. U.; Boxer, S. G.; Perry, J. W.; Marder, S. R. Studies of the Electronic Structure of Metallocene-Based Second-Order Nonlinear Optical Dyes. *J. Am. Chem. Soc.* **1999**, *121* (15), 3715–3723.
- (6) Di Bella, S. Second-Order Nonlinear Optical Properties of Transition Metal Complexes. *Chem. Soc. Rev.* **2001**, *30*, 355–366.
- (7) Coe, B. J.; Docherty, R. J.; Foxon, S. P.; Harper, E. C.; Helliwell, M.; Raftery, J.; Clays, K.; Franz, E.; Brunschwig, S. Syntheses and Properties of Salts of Chromophores with Ferrocenyl Electron Donor Groups and Quaternary Nitrogen Acceptors. *Organometallics* **2009**, *28*, 6880–6892.
- (8) Coe, B. J.; Fielden, J.; Foxon, S. P.; Asselberghs, I.; Clays, K.; Van Cleuvenbergen, S.; Brunschwig, B. S. Ferrocenyl Diquat Derivatives: Nonlinear Optical Activity, Multiple Redox States, and Unusual Reactivity. *Organometallics* **2011**, *30*, 5731–5743.
- (9) Kaur, P.; Kaur, M.; Depotter, G.; Van Cleuvenbergen, S.; Asselberghs, I.; Clays, K.; Singh, K. Thermally Stable Ferrocenyl “push–pull” Chromophores with Tailorable and Switchable Second-Order Non-Linear Optical Response: Synthesis and Structure–property Relationship. *J. Mater. Chem.* **2012**, *22* (21), 10597–10608.
- (10) Salman, S.; Brédas, J.-L.; Marder, S. R.; Coropceanu, V.; Barlow, S. Dipolar Ferrocene and Ruthenocene Second-Order Nonlinear Optical Chromophores: A Time-Dependent Density Functional Theory Investigation of Their Absorption Spectra. *Organometallics* **2013**, *32*, 6061–6068.
- (11) Zaarour, M.; Singh, A.; Latouche, C.; Williams, J. A. G.; Ledoux-Rak, I.; Zyss, J.; Boucekine, A.; Le Bozec, H.; Guerchais, V.; Dragonetti, C.; Colombo, A.; Roberto, D.; Valore, A. Linear and Nonlinear Optical Properties of Tris-Cyclometalated Phenylpyridine Ir(III) Complexes Incorporating π -Conjugated Substituents. *Inorg. Chem.* **2013**, *52*, 7987–7994.
- (12) Coe, B. J.; Foxon, S. P.; Helliwell, M.; Rusanova, D.; Brunschwig, B. S.; Clays, K.; Depotter, G.; Nyk, M.; Samoc, M.; Wawrzynczyk, D.; Garin, J.; Orduna, J. Heptametallic, Octupolar Nonlinear Optical Chromophores with Six Ferrocenyl Substituents. *Chem. - Eur. J.* **2013**, *19*, 6613–6629.
- (13) Coe, B. J. Developing Iron and Ruthenium Complexes for Potential Nonlinear Optical Applications. *Coord. Chem. Rev.* **2013**, *257*, 1438–1458.
- (14) Kaur, S.; Van Steerteghem, N.; Kaur, P.; Clays, K.; Singh, K. Diketopyrrolopyrrole Dyads: The Effect of Alkene. *J. Mater. Chem. C* **2016**, *4*, 9717–9726.
- (15) Coe, B. J.; Foxon, S. P.; Pilkington, R. A.; Sánchez, S.; Whittaker, D.; Clays, K.; Depotter, G.; Brunschwig, B. S. Nonlinear Optical Chromophores with Two Ferrocenyl, Octamethylferrocenyl, or 4-(Diphenylamino)phenyl Groups Attached to Ruthenium(I) or Zinc(II) Centers. *Organometallics* **2015**, *34*, 1701–1715.
- (16) Buckley, L. E. R.; Coe, B. J.; Rusanova, D.; Sánchez, S.; Jirásek, M.; Joshi, V. D.; Vávra, J.; Khobragade, D.; et al. Ferrocenyl Helquats: Unusual Chiral Organometallic Nonlinear Optical Chromophores. *Dalt. Trans.* **2017**, *46*, 1052–1064.
- (17) Kaur, S.; Kaur, M.; Kaur, P.; Clays, K.; Singh, K. Ferrocene Chromophores Continue to Inspire. Fine-Tuning and Switching of the Second-Order Nonlinear Optical Response. *Coord. Chem. Rev.* **2017**, *343*, 185–219.
- (18) Gray, H. B.; Sohn, Y. S.; Hendrickson, N. Electronic Structure of Metallocenes. *J. Am. Chem. Soc.* **1971**, *93* (15), 3603–3612.
- (19) Daeneke, T.; Kwon, T.; Holmes, A. B.; Duffy, N. W.; Bach, U.; Spiccia, L. Ferrocene-Based Electrolytes. *Nat. Chem.* **2011**, *3* (3), 211–215.
- (20) Ding, Y.; Zhao, Y.; Yu, G. A Membrane-Free Ferrocene-Based High-Rate Semiliquid Battery. *Nano Lett.* **2015**, *15*, 4108–4113.
- (21) El-zohry, A. M.; Cong, J.; Karlsson, M.; Kloos, L.; Zietz, B. Dyes and Pigments Ferrocene as a Rapid Charge Regenerator in Dye-Sensitized Solar Cells. *Dyes Pigm.* **2016**, *132*, 360–368.
- (22) Mi, Y.; Liu, W.; Yang, K. R.; Jiang, J.; Fan, Q.; Weng, Z.; Zhong, Y.; Wu, Z.; Brudvig, G. W.; Batista, V. S.; Zhou, H.; Wang, H. Ferrocene-Promoted Long-Cycle Lithium–Sulfur Batteries Angewandte. *Angew. Chem., Int. Ed.* **2016**, *55*, 14818–14822.
- (23) Beh, E. S.; De Porcellinis, D.; Gracia, R. L.; Xia, K. T.; Gordon, R. G.; Aziz, M. J. A Neutral pH Aqueous Organic–Organometallic Redox Flow Battery with Extremely High Capacity Retention. *ACS Energy Lett.* **2017**, *2*, 639–644.
- (24) Kaur, S.; Dhoun, S.; Depotter, G.; Kaur, P.; Clays, K.; Singh, K. Synthesis, Linear and Nonlinear Optical Properties of Thermally Stable Ferrocene-Diketopyrrolopyrrole Dyads. *RSC Adv.* **2015**, *5*, 84643–84656.
- (25) Misra, R.; Maragani, R.; Singh, C. P.; Chari, R. Dyes and Pigments Photonic Properties of Star Shaped Ferrocenyl Substituted Triazines. *Dyes Pigm.* **2016**, *126*, 110–117.
- (26) Mikhaylov, A.; Arias, E.; Moggio, I.; Ziolo, R.; Uudsemaa, M.; Trummal, A.; Cooper, T.; Rebane, A. Change of Electric Dipole Moment in Charge Transfer Transitions of Ferrocene Oligomers Studied by Ultrafast Two-Photon Absorption. *Proc. SPIE* **2017**, *10101*, 1010117.
- (27) Lakowicz, J. R. *Principles of Fluorescence Spectroscopy Principles of Fluorescence Spectroscopy*, 3rd ed.; Springer: Singapore, 2006.
- (28) Bublitz, G. U.; Boxer, S. G. Stark Spectroscopy: Applications in Chemistry, Biology, and Materials Science. *Annu. Rev. Phys. Chem.* **1997**, *48*, 213–242.
- (29) Barlow, S.; Marder, S. R. Electronic and Optical Properties of Conjugated Group 8 Metallocene Derivatives. *Chem. Commun.* **2000**, 1555–1562.
- (30) Jalviste, E.; Ohta, N. Stark Absorption Spectroscopy of Indole and 3-Methylindole. *J. Chem. Phys.* **2004**, *121* (10), 4730–4739.
- (31) Jackson, J. D. *Classical Electrodynamics*, 3rd ed.; John Wiley and Sons, Inc.: Hoboken, NJ, 1999.
- (32) Rebane, A.; Wicks, G.; Drobizhev, M.; Cooper, T.; Trummal, A.; Uudsemaa, M. Two-Photon Voltmeter for Measuring a Molecular Electric Field. *Angew. Chem., Int. Ed.* **2015**, *54* (26), 7582–7586.
- (33) Rebane, A.; Drobizhev, M.; Makarov, N. S.; Wicks, G.; Wnuk, P.; Stepanenko, Y.; Haley, J. E.; Krein, D. M.; Fore, J. L.; Burke, A. R.; Slagle, J. E.; McLean, D. G.; Cooper, T. M. Symmetry Breaking in Platinum Acetylide Chromophores Studied by Femtosecond Two-Photon Absorption Spectroscopy. *J. Phys. Chem. A* **2014**, *118* (21), 3749–3759.
- (34) Cooper, T. M.; Haley, J. E.; Krein, D. M.; Burke, A. R.; Slagle, J. E.; Mikhailov, A.; Rebane, A. Two-Photon Spectroscopy of a Series of Platinum Acetylides: Conformation-Induced Ground-State Symmetry Breaking. *J. Phys. Chem. A* **2017**, *121* (29), 5442–5449.
- (35) Terenziani, F.; Painelli, A.; Katan, C.; Charlot, M.; Blanchard-Desce, M. Charge Instability in Quadrupolar Chromophores: Symmetry Breaking and Solvatochromism. *J. Am. Chem. Soc.* **2006**, *128* (49), 15742–15755.
- (36) Dereka, B.; Rosspointner, A.; Li, Z.; Liska, R.; Vauthey, E. Direct Visualization of Excited-State Symmetry Breaking Using Ultrafast Time-Resolved Infrared Spectroscopy. *J. Am. Chem. Soc.* **2016**, *138* (13), 4643–4649.
- (37) Levitus, M.; Schmieder, K.; Ricks, H.; Shimizu, K. D.; Bunz, U. H. F.; Garcia-Garibay, M. A. Steps To Delineate the Effects of Chromophore Aggregation and Planarization in Poly-(phenyleneethynylene)s. 1. Rotationally Interrupted Conjugation in the Excited States of 1,4-Bis(phenylethynyl)benzene. *J. Am. Chem. Soc.* **2001**, *123* (18), 4259–4265.
- (38) Fujiwara, T.; Zgierski, M. Z.; Lim, E. C. Spectroscopy and Photophysics of 1,4-Bis(Phenylethynyl) Benzene: Effects of Ring

Torsion and Dark Pi Sigma* State Spectroscopy and Photophysics of 1, 4-Bis (Phenylethynyl) Benzene: Effects of Ring Torsion. *J. Phys. Chem. A* **2008**, *112*, 4736–4741.

(39) Roy, K.; Kayal, S.; Ariese, F.; Beeby, A.; Umopathy, S. Mode Specific Excited State Dynamics Study of Bis(phenylethynyl)benzene from Ultrafast Raman Loss Spectroscopy. *J. Chem. Phys.* **2017**, *146*, 064303.

(40) Roy, K.; Kayal, S.; Ravi Kumar, V.; Beeby, A.; Ariese, F.; Umopathy, S. Understanding Ultrafast Dynamics of Conformation Specific Photo-Excitation: A Femtosecond Transient Absorption and Ultrafast Raman Loss Study. *J. Phys. Chem. A* **2017**, *121* (35), 6538–6546.

(41) Levitus, M.; Garcia-Garibay, M. A. Polarized Electronic Spectroscopy and Photophysical Properties of 9,10-Bis-(phenylethynyl)anthracene. *J. Phys. Chem. A* **2000**, *104* (38), 8632–8637.

(42) Lin, C. J.; Kundu, S. K.; Lin, C. K.; Yang, J. S. Conformational Control of Oligo(p-Phenyleneethynylene)s with Intrinsic Substituent Electronic Effects: Origin of the Twist in Pentiptycene-Containing Systems. *Chem. - Eur. J.* **2014**, *20* (45), 14826–14833.

(43) Hurst, S. K.; Humphrey, M. G.; Morrall, J. P.; Cifuentes, M. P.; Samoc, M.; Luther-Davies, B.; Heath, G. A.; Willis, A. C. Organometallic Complexes for Nonlinear Optics Part 31. Cubic Hyperpolarizabilities of Ferrocenyl-Linked Gold and Ruthenium Complexes. *J. Organomet. Chem.* **2003**, *670*, 56–65.

(44) Dhoun, S.; Depotter, G.; Kaur, S.; Kaur, P.; Clays, K.; Singh, K. Thermally Stable Ferrocene-a-Cyanostilbenes as Efficient Materials for Second Order Nonlinear Optical Polarizability. *RSC Adv.* **2016**, *6*, 50688–50696.